Nanotechnology Perceptions
ISBN 1660-6795
www.nano-ntp.com

Friedel Oscillations in Schrödinger and Dirac Systems: Theory and Applications

Anmol Thakur,[1,*] Alok Kumar,[2] Upendra Kumar,[2] and Sarfaraz Khan[2]

[1] *Department of Physics, Jagdam College, Chapra, Saran, India 841301*
[2] *Department of Physics, Jai Prakash University, Chapra, India 841301*

Friedel oscillations are extensive spatial variations in electron density caused by impurities or faults within a Fermi system. They encode essential information regarding the fundamental Fermi surface, electronic dispersion, and scattering mechanisms. We explore the static desnity response function for massive and massless Dirac system in all three dimensions within random phase approximation. Further, we evaluate the Friedel oscillation for the same system in all three dimensions analytically. Our analytical results will be useful for exploring the use of massive Dirac materials as electrostatically tunable materials.

I. INTRODUCTION

Friedel oscillations (FOs), first predicted by Jacques Friedel in 1958[1], exemplify quantum mechanical interference among delocalized electrons caused by impurities and defects in materials, which are often inevitable in solid-state systems[2–5]. Friedel oscillations were initially detected by Crommie et al. in 1993 on the surface of copper. Utilizing scanning tunneling microscopy (STM), they revealed standing wave patterns arising from steps and point defects in the electrical local density of states[6–8]. By correlating the oscillation wavelength with electron energy, the investigation of Friedel oscillations has emerged as a potent method for elucidating the electronic band structures of novel and diverse materials[9–13].

FO result from the interference of electronic wavefunctions disrupted by impurities. Their wavelength is determined by the Fermi wave vector k_F, but their decay conveys information regarding dimensionality and dispersion[14–18]. Friedel oscillations have been detected on several surfaces, including metals and semiconductors, by the application of scanning tunneling microscopy (STM)[19–21]. Various fascinating characteristics of Friedel oscillations, including an unusually high oscillation amplitude and anisotropic oscillation wavelength, have been observed on Be (0 0 0 1) in the direction parallel to the surface[22]. FOs depend on the static density response of materials, which is analytically complex to compute. Despite the significant progress in materials science, particularly with the discovery of graphene, topological insulators, and Weyl semimetals, analytical formulations for the free energy in these systems remain limited and scarce.

In this paper, we study analytically the static density response functions for massive and massless Dirac systems in all three dimesnions. These response functions are further used for evaluating the long range desnity oscillations (FO) in the materials. As a begineer exercise, the static response function and FO for Schrodinger systems are derived before moving to Dirac systems. The aim of this work is to illustrate the key difference of the desnity oscillation on distance from the scatterer in one-, two-, and three dimesnional massive Dirac systems.

This article is organized as follows: In Sec. II, we introduce the theoretical formulation for obtaining the density response function of massive Dirac plamsa (MDP), and, parabolic dispersion systems. This allows us to evaluate the static limit of the response function and furter the FO in all three dimensions for the above-said systems. Next, using the above formalism, we calculate the FO for parabolic systems and MDP in Sec. III and Sec. IV respectively. Finally we conclude our findings in Sec. V.

* thakuranmol88@gmail.com

II. THEORETICAL FORMULATION FROM RESPONSE THEORY

In the random phase approximations (RPA), the collective plasmon modes of an electron system manifest as poles of the density-density response functions (also referred to as the polarization function or the Lindhard function) and align with the zeros of the complex longitudinal "dielectric function" $\epsilon(q,\omega)$, while its density oscillations induced by impurities are characterized by its static limit ($\omega \to 0$). The dielectric function is expressed as [23]

$$\epsilon(q,\omega) = \epsilon_0\{1 - v_q\Pi(q,\omega)\} = 0 \ , \tag{1}$$

where v_q is the Fourier transform of the Coulomb interaction, and $\Pi(q,\omega)$ is the total non-interacting polarizibility of the system. The Fourier transform of the Coulomb interaction $v(r) = e^2/(\kappa r)$, in the appropriate d-dimensional space is given by

$$v_q = \frac{4\pi e^2}{\kappa q^2} \qquad d = 3 \ , \tag{2a}$$

$$= \frac{2\pi e^2}{\kappa q} \qquad d = 2 \ , \tag{2b}$$

$$= \frac{2e^2}{\kappa} K_0(qa) \quad d = 1 \ , \tag{2c}$$

where κ is the background material dependent dielectric constant, and K_0 denotes the zeroth order modified Bessel function of the second kind. Note that in one dimension, the length scale a characterizes the lateral confinement size (say radius of the 1d ribbon), and $v_q \approx -2e^2\ln(qa)/\kappa$ for $qa \ll 1$, while $v_q = e^2/(\kappa q^2 a^2)$ for $qa \gg 1$.

In general, the polarization function for massive Dirac material is given by

$$\Pi(q,\omega) = \frac{g_s g_v}{L^d} \sum_{\mathbf{k},\lambda,\lambda'} F_{\lambda,\lambda'}(\mathbf{k},\mathbf{k}') \ \frac{n_{\rm F}(\lambda E_{\mathbf{k}}) - n_{\rm F}(\lambda' E_{\mathbf{k}'})}{\hbar\omega + \lambda E_{\mathbf{k}} - \lambda' E_{\mathbf{k}'} + i\eta} \ , \tag{3}$$

where $\mathbf{k}' = \mathbf{k} + \mathbf{q}$, $\lambda, \lambda' = \pm 1$ denotes the conduction (particle) and valence (hole) bands, $E_{\mathbf{k}} = \hbar v_{\rm F}|\sqrt{k^2 + (\Delta/\hbar v_{\rm F})^2}|$ with 2Δ being the energy gap, $n_{\rm F}(x)$ is the Fermi function and $2F_{\lambda,\lambda'}(\mathbf{k},\mathbf{k}') = 1 + \lambda\lambda'[\mathbf{k}\cdot\mathbf{k}' + \tilde{\Delta}^2]/(\tilde{E}_{\mathbf{k}}\tilde{E}_{\mathbf{k}'})$ is the overlap function, with $\tilde{x} \equiv x/\hbar v_{\rm F}$. The factor g_s (= 2) is the spin degeneracy factor and g_v is the valley (or pseudo spin) degeneracy factor (e.g. $g_v = 2$ for graphene and other Dirac materials with honeycomb lattice structure). Considering the relation $\Pi(q,-\omega) = \Pi(q,\omega)^*$ and the dependence of the polarization function solely on the absolute value of the Fermi energy $\varepsilon_{\rm F}$, we restrict our presentation to results for $\varepsilon_{\rm F} > 0$ and $\omega > 0$. Additionally, we operate at absolute zero temperature, allowing the substitution of Fermi functions with Heaviside step functions, specifically, $n_{\rm F}(x) = \Theta(\varepsilon_{\rm F} - x)$.

Based on the position of the Fermi energy $\varepsilon_{\rm F}$, the polarization function can be divided into two components: intrinsic polarization for $\varepsilon_{\rm F} < \Delta$ and extrinsic polarization for $\varepsilon_{\rm F} > \Delta$.

$$\begin{aligned}\Pi\ (q,\omega) &= -\chi^-_\infty(q,\omega) + \underbrace{\chi^-_{\varepsilon_{\rm F}}(q,\omega) + \chi^+_{\varepsilon_{\rm F}}(q,\omega)} \\ &= \Pi_0(q,\omega) + \theta(\varepsilon_{\rm F} - \Delta)\ \Pi_1(q,\omega) \ ,\end{aligned} \tag{4}$$

where

$$\chi^{\pm}_D(q,\omega) = -\frac{g_s g_v}{(2\pi)^d} \int d^dk \ \Theta(D^2 - \Delta^2 - k^2) \tag{5}$$

$$\times \left(1 \pm \frac{\mathbf{k}\cdot\mathbf{k}' + \tilde{\Delta}^2}{\tilde{E}_{\mathbf{k}}\ \tilde{E}_{\mathbf{k}'}}\right) \left[\frac{E_{\mathbf{k}} \mp E_{\mathbf{k}'}}{(\hbar\omega + i\eta)^2 - (E_{\mathbf{k}} \mp E_{\mathbf{k}'})^2}\right] \ .$$

Here the upper and lower signs correspond to intraband and interband electron-hole transitions respectively and the parameter D defines the integration limits via the Θ function.

Once the non-interacting density-density response function is known, the collective density excitations (plasmon modes) are given by the poles of the interacting density-density response function.

The static limit of the polarization function $\Pi(q,0)$ is useful for determining the screened Coulomb potential of a charged impurity. The induced charge density in the system due to the potential of an impurity with charge Ze located at a distance d infront of the system is given by [24]

$$\delta n(r) = Ze \int \frac{\mathrm{d^d q}}{2\pi^d} e^{-qd} \left[\frac{1}{\epsilon(q,0)} - 1\right] \exp(i\vec{q}\cdot\vec{r}) \tag{6}$$

where $\epsilon(q,\omega)$ is the longitudnal di-electric constant. Upon integrating over the angular part we can write the expression in Eq. (6) in compact form as

$$\delta n(r) = \int_0^\infty \left[\frac{1}{\epsilon(q,0)} - 1\right] F_d(qr) q^{q-1} \mathrm{dq} \tag{7}$$

where

$$\begin{aligned} F_d(x) &= \frac{\cos(x)}{\pi}, 1D \\ &= \frac{J_0(x)}{2\pi}, 2D \\ &= \frac{\sin(x)}{x}, 3D \ . \end{aligned}$$

In the next sections, we evaluate the Fridel oscillations for parabolic and Dirac systems from the theroy developed above.

III. STATIC POLARIZATION FUNCTION AND FRIDEL OSCILLATION FOR PARABOLIC DISPERSION

For parabolic dispersion with energy dispersion $E_k = \hbar^2 k^2/2m$, in static limit ($\omega = 0$), Eq. (3) in all three dimension reduces to where k_f is the Fermi momentum. Plots for polarization function in all three

dimension	$\tilde{\Pi}(q,0)$
1D	$\frac{k_f}{q} \log \frac{q+2k_f}{q-2k_f}$
2D	$1 - \theta(q-2k_f)\frac{\sqrt{q^2-4k_f^2}}{q}$
3D	$\frac{1}{2} + \frac{q^2-4k_f^2}{8qk_f} \log \frac{q-2k_f}{q+2k_f}$

TABLE I: Expressions for $\Pi(q,0)$ for parabolic system in all three dimensions

dimensions shows that the Lindhard function is singular at $q = 2k_f$. For three and two dimensios the singularity appears in the second and first derivative of $\Pi(q,0)$ respectively, whereas in one dimension the function itself has a logrithmic divergence. The screened potential corresponding to Eq. (6) is given by

$$\phi(r) = Ze \int \frac{\mathrm{d^d q}}{(2\pi)^d} \frac{e^{i\mathbf{qr}} v(q)}{\epsilon(q,0)} e^{-qd} \tag{8}$$

where d is the distance above the plane where the charge is kept. For solving above integral in all dimension, we will make use of **Riemann–Lebesgue lemma**, which states that if a function oscillates rapidly around zero then the integral of this function is small and the principal contribution to the integral is determined by the integrand behavior in the neighborhood of singular points. Since $\epsilon(q,0)$ is singular at $q = 2k_f$ in all dimensions, upon expanding the dielectric function around $q = 2k_f$ the integrand reduces to

$$\frac{1}{\epsilon(q,0)} \sim \frac{v_{2k_f} \partial\Pi(\kappa)}{\epsilon_o[1 - v_{2k_f}\Pi(2k_f)]^2} \tag{9}$$

substituting above expression in Eq. (8) we get,

$$\phi(r) = A^d(2k_f) \int \partial\Pi(\kappa) S(\kappa) e^{-\kappa d} \tag{10}$$

where $v^d(q)$ is the Fourier transform of Coulumb potential in d dimension, $A^d(2k_f) = Ze\epsilon_0 \frac{k_f^{d-1} v_{2k_f}^d e^{-2k_f d}}{(2\pi)^d \epsilon_o [1 - v_{2k_f}^d \Pi^d(2k_f)]^2}$ is a dimension dependent constant, $\partial\Pi(\kappa) = \Pi(2k_f + \kappa)$ and $S(\kappa)$ is defined as

$$\begin{aligned} S(\kappa) &= \frac{\sin(2k_f + \kappa)r}{k_f r}, 3D \\ &= \frac{2\pi \cos\{(2k_f + \kappa)r - \pi/4\}}{\sqrt{2k_f r}}, 2D \\ &= \cos(2k_f + \kappa)r, 1D \end{aligned} \tag{11}$$

Using the above expressions the potential in all three dimensions are given as .

dimension	$\phi(r)$
1D	$A^1(2k_f)\frac{\pi \cos(2k_f r)}{r}$
2D	$A^2(2k_f)\frac{\sin(2k_f r)}{r^2}$
3D	$A^3(2k_f)\frac{\sin(2k_f r)}{r^3}$

TABLE II: Analytical expressions of $\phi(r)$ for parabolic system in all three dimensions

In the next section, we use the theoretical formalism developed above to evaluate the FO in MDP in all three dimensions.

IV. FRIEDEL OSCILLATIONS IN MASSIVE AND MASSLESS DIRAC SYSTEM

In this section, we calculate and present the full analytical expression of the static polarization function for massive Dirac sysems in one, two, and three dimensions. The expressions for static functions are further used for the evaluation of FO in all systems.

A. 1D massive system

For 1d gapped Dirac materials, the static part of intrinsic polarization function is given by

$$\Pi_0^{(1d)} = \frac{g}{\pi}\left[-1 - \frac{2\tilde{\Delta}^2}{q\sqrt{q^2 + 4\tilde{\Delta}^2}} \log\left(\frac{\sqrt{q^2 + 4\tilde{\Delta}^2} - q}{\sqrt{q^2 + 4\tilde{\Delta}^2} + q} \right) \right], \tag{12}$$

and the extrinsic part is given by

$$\Pi_1^{(1d)} = -\frac{g}{\pi} \frac{2\tilde{\Delta}^2}{q\sqrt{q^2 + 4\tilde{\Delta}^2}} \left[\log\left(\frac{(q + 2k_F)\beta_1(k_F)}{|q - 2k_F|\beta(-k_F)} \right) \right], \tag{13}$$

where $\beta_1(k_F) = k_F q + 2\tilde{\Delta}^2 + \sqrt{(k_F^2 + \tilde{\Delta}^2)(q^2 + 4\tilde{\Delta}^2)}$. Once again we can observe the logarithmic divergence at $q = 2k_f$ in extrinsic reponse function. The oscillations in potential due to the anomalies at $q = 2k_f$ is given by

$$\phi(r) \approx A^1(2k_f) \frac{\Delta^2 \cos(2k_f r)}{r} \tag{14}$$

As evident from the above expression, the FO for massless ($\Delta = 0$) systems vanishes in 1D which is a consequence of the fact that perfect backscattering or mixing of different chirality fermions in one dimension is forbidden.

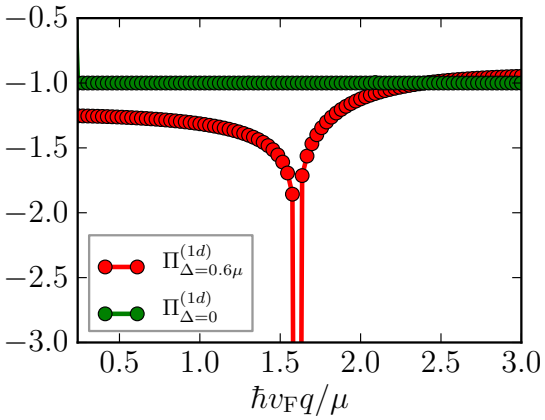

(a)

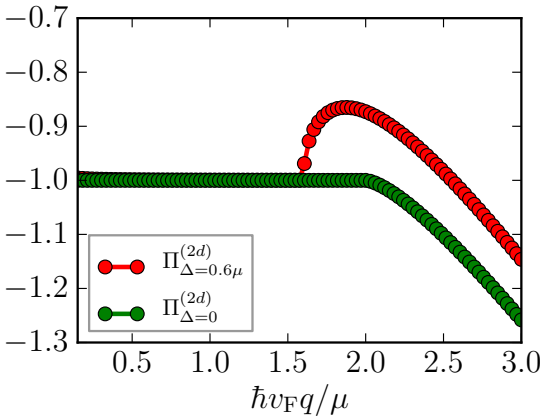

(b)

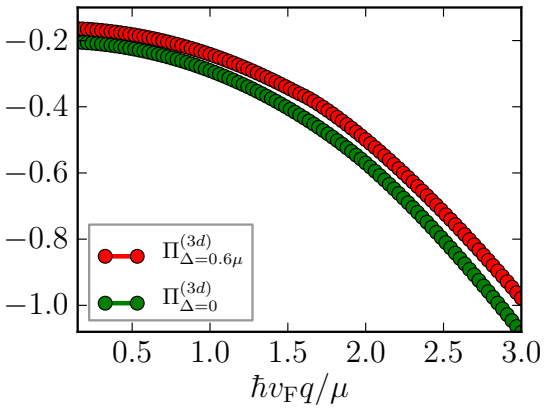

(c)

FIG. 1: (Color online) Comparison of the static polarization for massless and massive Dirac materials in (a) 1D, where discontinuity appears in the static polarizatin itself (b) 2D, where discontinuity appears in the first derivative of static polarization function (c) 3D, where discontinuity appears in the second derivative of static polarization function and

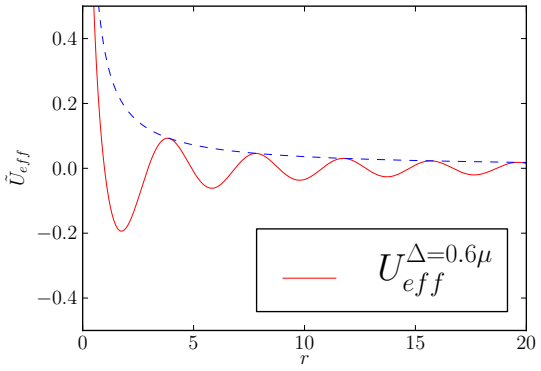

(a)

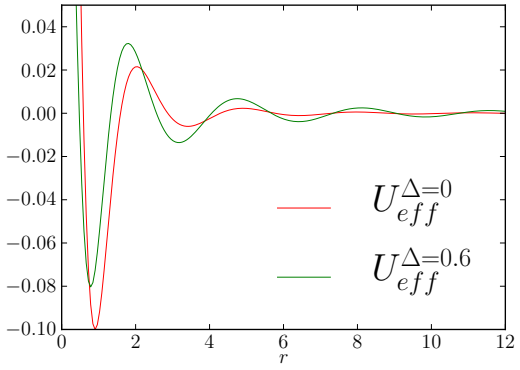

(b)

FIG. 2: (Color online) Effective FO in potential vs the distance of the scatterer for a) 1D massive Dirac system b) 2D massive and massless Dirac systems.

B. 2D massive and massless Dirac system

For two dimensional gapped system with linear dispersion, the static polarization function is given by [24]

$$\Pi_1^{(2d)}(q,0) = \frac{g\tilde{\mu}}{\pi}\left[1-\theta(q-2k_f)\left(\frac{\sqrt{q^2-4k_f^2}}{2q} - \frac{q^2-4\tilde{\Delta}^2}{4q\tilde{\mu}}\arctan\frac{\sqrt{q^2-4k_f^2}}{2\tilde{\mu}}\right)\right].$$

The induced potential in this case is given by

$$\phi(r) \approx A^2(2k_f)\alpha\frac{\sin 2k_f r}{r^2} \tag{15}$$

where $\alpha = \frac{1}{2\sqrt{k_f}}\left(1-\frac{k_f^2-\Delta^2}{\mu^2}\right)$. One thing to be noted here that for gapless 2d system i,e graphene, $\alpha \to 0$ and then the second order term from the expnasion of $\arctan(\sqrt{k_f^{-1}\kappa})$ contributes. In that case the induced potential is given by

$$\phi(r,\Delta=0) \approx A^2(2k_f)\frac{\sin 2k_f r}{r^3} \tag{16}$$

C. 3D massive and massless Dirac Systems

For masless 3d Dirac system, the static polarization function is given by [24]

$$\Pi(q,0) = \frac{2}{3}\left[1 + \frac{k_f}{2q}\left(1 - \frac{3q^2}{4k_f^2}\right)\log\left(\frac{q+2k_f}{q-2k_f}\right) - \frac{q^2}{8k_f^2}\log\left(\frac{4k_f^2-q^2}{q^2}\right) + \frac{q^2}{4k_f^2}\log\left(\frac{\lambda}{q}\right)\right]$$

where λ represents the large momentum cutoff. In this case the induced potential is given as

$$\phi(r) \approx A^3(2k_f)\frac{\sin(2k_f r)}{r^4} \tag{17}$$

The analytical expressions for the static polarization function of massive Dirac system is beyound the scope of this paper. However, numerical results are shown in the figure.

V. EXPERIMENTAL OBSERVATIONS AND COCLUSIONS

To summarize, we have calculated the exact one-loop static polariza- tion function for massive as well as massless Dirac systems in 1d, 2d and 3d. The calculated polarization function is then used to obtain the screened potential of a localized impurity. Additionally using the exact polarization function in the static limit, we find that the Friedel oscillations in a massive Dirac system decay as r^{-2} and r^{-3} in 2d and 3d respectively similar to the case of para- bolic dispersion and unlike the massless Dirac case where the corresponding Friedel oscillations decay as r^{-3}. STM and scanning tunneling spectroscopy (STS) provide direct access to Friedel oscillations by imaging LDOS modulations around impurities. Quasiparticle interference patterns in Fourier-transformed STM data reveal scattering vectors and Fermi surface geometry. For example in graphene, STM studies confirmed the suppression of $2k_F$ backscattering.[25] instead of conventional oscillations, weaker and faster-decaying modulations were observed.

We anticipate that our analytical findings on the polarization function, plasmon dispersion, and Friedel oscillations will facilitate the investigation of the physics of both massive and massless Dirac electrons across diverse experimental systems with varying dimensionality. An advantageous extension of our research will involve incorporating finite temperature effects into the computation of the polarization function.

ACKNOWLEDGMENTS

We acknowledge insightful discussions with V. Singh and support from RUSA, Bihar for technical support.

[1] J. Friedel, Philos. Mag. **43**, 153 (1952).
[2] Bäcker, A. and Dietz, B. and Friedrich, T. and Miski-Oglu, M. and Richter, A. and Schäfer, F. and Tomsovic, S. Phys. Rev. B. **80**, 066210 (2009).
[3] Simion, George E. and Giuliani, Gabriele F. Phys. Rev. B. **72** 045127 (2005)
[4] Farajollahpour, T., Khamouei, S., Shateri, S.S. et al. Scientific Reports **8** 2667 (2018)
[5] Sessi, P., Silkin, V., Nechaev, I. et al. Nat. Comm. **6** 8691 (2015)
[6] Hofmann, Ph. and Briner, B. G. and Doering, M. and Rust, H.-P. and Plummer, E. W. and Bradshaw, A. M. Phys. Rev. Lett. **79**, 265 (1997)
[7] M. F. Crommie, C. P. Lutz, and D. M. Eigler Nature **363** 524 (1993)
[8] M. F. Crommie, C. P. Lutz, and D. M. Eigler Science **262** 218 (1993)
[9] Würsch, C., Stamm, C., Egger, S. et al. Nature **389** 937 (1997)
[10] Jian Chen and Huai-Zhe Xu 2015 Commun. Theor. Phys. **64** 108 (2015)
[11] Jia-Jun Tang et al 2014 J. Phys. D: Appl. Phys. **47** 115305 (2014)
[12] F Gleisberg et al 2001 J. Phys. B: At. Mol. Opt. Phys. **34** 4645 (2001)
[13] Mahmoud M Asmar and Wang-Kong Tse 2022 J. Phys.: Condens. Matter **34** 315602 (2022)
[14] Joy Prakash Das et al 2020 Phys. Scr. **95** 075710 (2020)
[15] S N Artemenko et al 2004 J. Phys. B: At. Mol. Opt. Phys. **37** S49 (2004)

[16] Feibelman, Peter J. Phys. Rev. B. **55** 8821 (1997)
[17] Hofmann, Ph. and Briner, B. G. and Doering, M. and Rust, H.-P. and Plummer, E. W. and Bradshaw, A. M. Phys. Rev. B. **79** 265 (1997)
[18] Rensink, Marvin E. Phys. Rev. B. **174** 744 (1968)
[19] Zhang, J. M. and Liu, Y. Phys. Rev. B. **97** (2018)
[20] Sadhukhan, Krishanu and Agarwal, Amit Phys. Rev. B **96**, 035410 (2017)
[21] Sachdeva, Rashi and Thakur, Anmol and Vignale, Giovanni and Agarwal, Amit Phys. Rev. B **91**, 205426 (2015)
[22] E. W. Plummer, E. Laegsgaard, L. Petersen, and F. Besenbacher Phys. Rev. Lett. **79** 265 (1997)
[23] "Quantum Theory of the Electron Liquid", Gabriele F. Giuliani and Giovanni Vignale, Cambridge University Press, *ISBN: 978-0521527965* (2005)
[24] Thakur. A. et al 2017 J. Phys.: Condens. Matter **29** 105701 (2017)
[25] C. Bena, Phys. Rev. Lett. **100**, 076601 (2008).